Geophysical Research Letters

Dissolved Organic Nitrogen Production and Export by Meridional Overturning in the Eastern Subpolar North Atlantic

Bieito Fernández-Castro[1,2], Marta Álvarez[3], Mar Nieto-Cid[3], Patricia Zunino[4], Herlé Mercier[4], and Xosé Antón Álvarez-Salgado[1]

[1]Departamento de Oceanografía, Instituto de Investigacións Mariñas (IIM-CSIC), Vigo, Spain, [2]Physics of Aquatic Systems Laboratory, Margaretha Kamprad Chair, Ecole Polytechnique Fédérale de Lausanne, Institute of Environmental Engineering, Lausanne, Switzerland, [3]Centro Oceanográfico de A Coruña, Instituto Español de Oceanografía, A Coruña, Spain, [4]Laboratoire d'Océanographie Physique et Spatiale, UMR 6523 CNRS/Ifremer/IRD/UBO, Ifremer Centre de Bretagne, Plouzané, France

Abstract Dissolved organic matter (DOM) is produced in the surface and exported towards the deep ocean, adding ∼ 2 PgC/year to the global carbon export. Due to its central role in the Meridional Overturning Circulation, the eastern subpolar North Atlantic (eSPNA) contributes largely to this export. Here we quantify the transport and budget of dissolved organic nitrogen (DON) in the eSPNA, in a box delimited by the OVIDE 2002 section and the Greenland-Iceland-Scotland sills. The Meridional Overturning Circulation exports >15.9 TgN/year of DON downward and, contrary to the extended view that these are materials of subtropical origin, up to 33% of the vertical flux derives from a net local DON production of 7.1 ± 2.6 TgN/year. The low C:N molar ratio of DOM production (7.4 ± 4.1) and the relatively short transit times in the eSPNA (3 ± 1 year) suggest that local biogeochemical transformations result in the injection of fresh bioavailable DOM to the deep ocean.

1. Introduction

Dissolved organic matter (DOM) represents one of the largest reservoirs of reduced carbon on Earth (662 PgC; Hansell et al., 2009). The production of DOM occurs primarily in the euphotic zone as a result of phytoplankton photosynthesis and subsequent food web interactions (Carlson, 2002). While labile DOM is remineralized within the source region, recalcitrant DOM (including the semilabile, semirefractory, and refractory fractions; Hansell, 2013) escapes rapid degradation and can be transported horizontally by ocean currents (Letscher et al., 2013; Torres-Valdés et al., 2009) or exported downward by convergence in subtropical regions (Hansell et al., 2012), winter convection (Carlson et al., 1994), and overturning circulation (Carlson et al., 2010; Fontela et al., 2016). Globally, 1.9 PgC/year of recalcitrant DOM are exported to the deep ocean (Hansell et al., 2009), contributing 15–38% to the global carbon export (5–12 PgC/year; Henson et al., 2011), and fueling heterotrophic respiration in the dark ocean (Carlson et al., 2010; Hansell et al., 2012).

The subpolar North Atlantic (SPNA) is a key region for the Meridional Overturning Circulation (MOC) (Daniault et al., 2016). The North Atlantic Current (NAC) carries warm and saline thermocline waters of subtropical origin into the SPNA gyre along its southeastern rim, constituting the northward flowing upper limb of the MOC in the region (Figure 1a). Subtropical waters progressively gain density through air-sea exchange and are transformed into subpolar mode waters (SPMW; Brambilla & Talley, 2008; García-Ibáñez et al., 2015), whose densest variety is the Irminger SPMW (Krauss, 1995; García-Ibáñez et al., 2015). Deep convection in the Irminger Sea (Pickart et al., 2003; Piron et al., 2017) and Labrador Sea (Yashayaev et al., 2007) leads to the formation of the Labrador Sea Water (McCartney & Talley, 1982). These water masses, together with the Denmark Strait Overflow Water (DSOW) and Iceland-Scotland-Overflow Water (ISOW), which enter the eastern SPNA (eSPNA) from the Arctic and Nordic Seas through the Denmark and Iceland-Scotland Straits (Jochumsen et al., 2017; Macrander et al., 2005; Nilsson et al., 2008), respectively, compose the southward flowing lower limb of the MOC.

The northward flowing DOM-rich waters of subtropical origin sink in the SPNA and return southward into the deep North Atlantic brought by the MOC (Fontela et al., 2016; Hansell et al., 2009). Subsequent to this
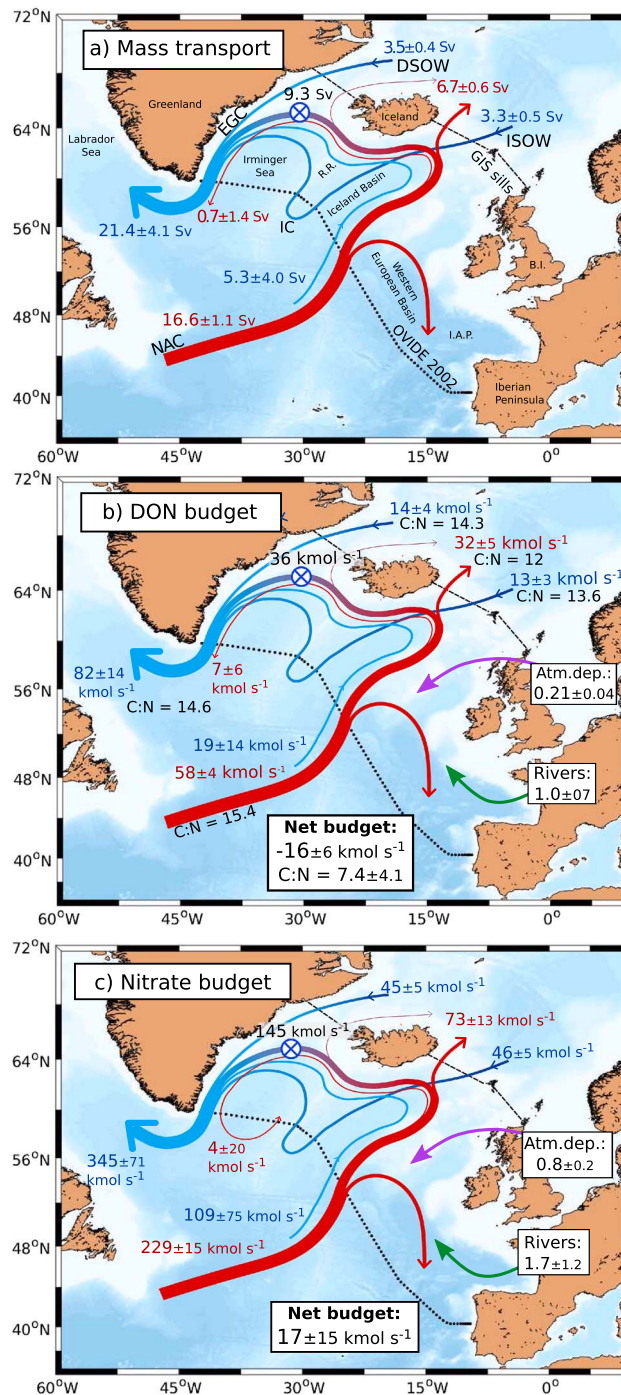
Figure 1. Map of the study area in the eastern subpolar North Atlantic and (a) volume transports (1 Sv = 10^6 m^3/s) across the OVIDE 2002 section and the Greendland-Iceland-Scotland (GIS) sills, (b) dissolved organic nitrogen (DON), and (c) nitrate transports and net budget (kmol/s). Red (upper) and blue (lower) arrows and numbers represent the circulation in the density levels corresponding to the upper and lower limbs of the Atlantic Meridional Overturning Circulation, limited by the σ_1 = 32.15-kg/m^3 isopycnal. NAC, IC, and EGC represent the North Atlantic, Iceland, and East Greenland Currents. DSOW and ISOW are the Denmark Strait and Iceland Strait overflows. R.R. is the Reikjanes Ridge, and I.A.P. is the Iberian Abyssal plain. Fluxes across the OVIDE 2002 section are given for the Irminger Sea plus Iceland Basin (west) and Western European Basin (east). Fluxes across the GIS sills are reported for the DSOW, the ISOW (blue), and the Atlantic Water (plus Polar Water; red). The $\otimes$ symbol represents the downward transport by the overturning circulation. The supply by atmospheric deposition and rivers is represented by the purple and green arrows, respectively. In panel (b), the C:N molar ratios, calculated as the ratio of the dissolved organic carbon and DON transports and budget, are shown in black font.

export, removal of the semirefractory fraction of this DOM has been documented in the deep North Atlantic Ocean (Carlson et al., 2010; Hansell et al., 2012; Fontela et al., 2016). However, these studies did not discuss the role of the SPNA as a source or sink of DOM (Carlson et al., 2010; Hansell et al., 2012), or they considered that the DOM imported from the thermocline waters of subtropical origin does not suffer significant biogeochemical transformations in the SPNA and it is only passively transported to the deep ocean by the MOC (Fontela et al., 2016). More recently, a diagnostic modeling study suggested instead that the production and export of DOM to the deep ocean are tightly coupled in the high-latitude North Atlantic Ocean (Roshan & DeVries, 2017). Furthermore, all these studies have focused on dissolved organic carbon (DOC), while it has been shown that the transport and remineralization of dissolved organic nitrogen (DON) is central to understand the biogeochemical nutrient budgets, both in low-latitude and polar regions (Letscher et al., 2013; Torres-Valdés et al., 2009; Torres-Valdés et al., 2016; Vidal et al., 2018).

Here we evaluate the transports and net budget of DON in the eSPNA to investigate the net production of DON along the transit through the subpolar gyre and its subsequent export by the lower limb of the MOC. In order to assess the biogeochemical relevance of the DON transports and budgets, equivalent calculations were performed for DOC and nitrate.

2. Methods

2.1. Nutrient Budgets in the eSPNA

The budgets of DON, DOC, and nitrate in the eSPNA were determined within a box delimited by the Greenland-Portugal OVIDE 2002 section to the southwest and the Greenland-Iceland-Scotland (GIS) sills to the northeast. The box has a surface area of 3.74×10^{12} m^2 and a volume of 7.96×10^{15} m^3. The rate of change of an organic or inorganic nutrient N ($\partial N/\partial t$) in the eSPNA box is the sum of net transport across the OVIDE 2002 section ($T_N^{\text{Ov.,0}}$, where Ov. stands for the OVIDE 2002 section and the 0 superscript is to specify that volume-conserving transports are used, see below) and the GIS sills ($T_N^{\text{Sills.,0}}$), the input from rivers (F_N^{rivers}) and atmospheric deposition ($F_N^{\text{at.dep.}}$) and a rate of net biological production (J_N^{BG}):

$$\frac{\partial N}{\partial t} = T_N^{\text{Ov.,0}} - T_N^{\text{Sills,0}} + F_N^{\text{rivers}} + F_N^{\text{at.dep.}} + J_N^{BG}. \tag{1}$$

As oceanic volume transports are defined positive to the north, a minus sign was added for the transports across the GIS sills (northward fluxes are out of the box). The net production rate (J_N^{BG}) was diagnosed from the balance of oceanic, riverine, and atmospheric fluxes by assuming steady state ($\partial N/\partial t = 0$). The nutrient transports across the southern boundary of the eSPNA were calculated by combining volume transports derived from an inverse model applied to hydrographic measurements (Lherminier et al., 2007) and nutrient concentration measurements (Álvarez-Salgado et al., 2013) along the OVIDE 2002 section. Transports across the northern boundary, Greenland-Iceland-Scotland (GIS) sills, and the atmospheric and riverine inputs were evaluated using data from the literature and public databases.

2.2. Nutrient Transports Across the OVIDE 2002 Section

The cruise OVIDE 2002 was conducted from 19 June to 11 July 2002, on board R/V Thalassa. Ninety-one full-depth hydrographic stations were occupied, from the continental shelf off Greenland to Lisbon. Nitrate profiles from Niskin bottle data were obtained at every station (maximum 30 pressure levels). DON and DOC data were determined at 30 stations and selected depths (maximum 15 levels). The analytical determination error was ± 0.1, ± 0.32, and $\pm 0.7 \mu$mol/kg for nitrate, DON, and DOC. Nitrate concentrations have been adjusted by applying a multiplicative factor of 0.96 according to the GLODAPv2 adjustment table (https://glodapv2.geomar.de/). A detailed description of the instruments and calibrations associated with the physical and chemical parameters are presented elsewhere (Lherminier et al., 2007; Álvarez-Salgado et al., 2013).

The absolute transport of an organic or inorganic nutrient N across the OVIDE 2002 section can be computed as

$$T_N = \int_{\text{Greenland}}^{\text{Portugal}} \int_{\text{bottom}}^{\text{surface}} \rho(x,z) N(x,z) V(x,z) \, dx \, dz, \tag{2}$$

where V is the velocity orthogonal to the section and ρ is the in situ density. Transports were defined positive to the north. The velocity field was calculated by combining geostrophic currents and acoustic Doppler

current profiles in an inverse generalized least squares method. The specifications of the method for the OVIDE 2002 cruise and the description of current field are detailed elsewhere (Lherminier et al., 2007). The volume transports were estimated at the middistance between two stations with a vertical resolution of 1 dbar, and nutrient concentrations were obtained at each sampling point (i.e. bottle depth) for each hydrographic station. In order to match the grid of both fields, the nutrient fields were linearly interpolated at each 1 dbar and averaged in station pairs. The DOC and DON samples, collected in one out of three stations, were linearly interpolated in the horizontal coordinate to each station position prior to vertical interpolation. The cross-section velocity, nitrate, and DON fields are shown in supporting information Figure S1.

In order to diagnose net biogeochemical rates from the nutrient budgets in the eSPNA box, mass conservation must be ensured in the boxed region. To meet this requirement, nutrient transports were decomposed into fluxes associated with the net volume transport across the section ($T_{\mathrm{N}}^{\mathrm{Ov., Net}}$) and the volume-conserving fluxes ($T_{\mathrm{N}}^{\mathrm{Ov., 0}}$) (Zunino et al., 2014), $T_{\mathrm{N}}^{\mathrm{Ov.}} = T_{\mathrm{N}}^{\mathrm{Ov., Net}} + T_{\mathrm{N}}^{\mathrm{Ov., 0}}$, by splitting the cross-section velocity (V) into two components,

$$V(x,z) = \overline{V} + v(x,z), \tag{3}$$

where $\bar{V}$ is the section-averaged velocity corresponding to the net transport across the section:

$$T_{\mathrm{Vol}}^{\mathrm{Ov., Net}} = \bar{V} \int \int \mathrm{d}x\,\mathrm{d}z. \tag{4}$$

With this, the volume-conserving nutrient fluxes were calculated as the product of the nutrient concentrations and the velocity anomalies along the section:

$$T_N^{\mathrm{Ov., 0}} = \int\limits_{\mathrm{Greenland}}^{\mathrm{Portugal}} \int\limits_{\mathrm{bottom}}^{\mathrm{surface}} \rho(x,z) N(x,z) v(x,z) \,\mathrm{d}x\,\mathrm{d}z. \tag{5}$$

The net volume transport across the OVIDE 2002 was small ($T_{\mathrm{Vol}}^{\mathrm{Ov., Net}} = -0.03 \pm 2.85$ Sv) and southward. The nutrient fluxes associated with this net volume transport, calculated as $T_{\mathrm{N}}^{\mathrm{Ov., Net}} = \overline{\rho N}\, T_{\mathrm{Vol}}^{\mathrm{Ov.,Net}}$, where $\overline{\rho N}$ is the section-averaged volumetric nutrient concentration, were -0.5 ± 51.5 kmol/s for nitrate, -0.1 ± 9.8 kmol/s for DON, and -1.4 ± 141 kmol/s for DOC.

For display purposes, the transports were also divided in the contributions of the upper and lower limbs of the MOC, separated by the $\sigma_1 = 32.15$ kg/m^3 potential density level (referenced to 1,000 m). Errors in the transports were calculated as the standard deviation of 1,000 realizations generated by random perturbations of the velocity and nutrient fields based on the covariance matrix of the reference velocities (Lherminier et al., 2007) and the nutrient measurement errors (Álvarez-Salgado et al., 2013).

2.3. Transports Across the GIS Sills

The nutrient transports across the GIS sills were calculated as the product of the volume transport of the water masses present at the GIS sills ($n = 7$) and an averaged nutrient concentration for the corresponding water mass (N^i):

$$T_N^{\mathrm{Sills}} = \sum_{i=1}^{7} T^i{}_{\mathrm{Vol}} \rho^i N^i. \tag{6}$$

Volume transports at the GIS sills were available from literature (Hansen et al., 2008; Jeansson et al., 2011; Østerhus et al., 2005; Table S1). Briefly, 0.8 ± 0.16 Sv of Atlantic Water (AW) and 1.5 ± 0.5 Sv of Polar Water (PW) flow northward and southward (Nilsson et al., 2008; Østerhus et al., 2005), respectively, in the upper density levels of the Denmark Strait (DS), while -3.4 ± 0.4 Sv of dense DSOW flow southward (Macrander et al., 2005). In the Iceland-Faroe Ridge, 3.8 ± 0.5 Sv of AW flow northward (Østerhus et al., 2005) and -1.0 ± 0.5 Sv of ISOW flow southward (Hansen et al., 2008). Finally, 3.8 ± 0.5 Sv of AW cross the Faroe-Shetland Channel to the north (Østerhus et al., 2005) and -2.1 ± 0.3 Sv of ISOW enter the subpolar North Atlantic (Hansen et al., 2008).

Similarly to the OVIDE 2002 section, the net nutrient transports were decomposed into the fluxes associated with the net transport of volume across the sills ($T_{\mathrm{Vol}}^{\mathrm{Sills, Net}} = 0.4 \pm 1.2$ Sv) and the volume-conserving flux.

In order to calculate the latter, the volume transports by each water mass with no net associated volume transport across the GIS sills were calculated as $T_{\mathrm{Vol}}^{i,0} = T_{\mathrm{Vol}}^{i} - T_{\mathrm{Vol}}^{\mathrm{Sills,\,Net}}/7$. Volume-conserving fluxes, which differ only slightly from the total fluxes in Table S1, are used throughout the manuscript. Thus, the flux of a nutrient corresponding to a net zero volume transport was

$$T_N^{\mathrm{Sills,0}} = \sum_{i=1}^{7} T_{\mathrm{Vol}}^{i,0} \rho^i N^i. \tag{7}$$

Nitrate concentrations at the sills were obtained from the World Ocean Atlas 2013 (https://www.nodc.noaa.gov/OC5/woa13/), and DOC concentrations were available in Jeansson et al. (2011). DON concentrations in the AW, DSOW, and ISOW were obtained by extrapolating the mean DON in these water masses (i) along the OVIDE 2002 section (Álvarez-Salgado et al., 2013), taking into account the removal of DON from the sills to the section:

$$\mathrm{DON}^{i,\,\mathrm{Sills}} = \mathrm{DON}^{\mathrm{Ov.}} + (1/r_{\mathrm{CN}})(\mathrm{DOC}^{i,\,\mathrm{Sills}} - \mathrm{DOC}^{\mathrm{Ov.}}), \tag{8}$$

where r_{CN} is the C:N molar ratio of DON removal in the eSPNA and $r_{\mathrm{CN}} = 6.9 \pm 0.6$ for basin-scale remineralization (Álvarez-Salgado et al., 2013). The correspondence between the water masses in the OVIDE 2002 section and the GIS sills and the calculated DON concentrations are given in Table S1. The PW was not intercepted in the OVIDE 2002 section. In order to obtain its DON concentration, the DOC value given by Jeansson et al. (2011) was divided by 14, a typical C:N ratio for bulk concentrations of DOM in upper and thermocline waters in the area (Álvarez-Salgado et al., 2013). To the best of our knowledge, the only available measurements of DON in the area of the GIS sills were carried out in the East Greenland Current (EGC) across the DS (Torres-Valdés et al., 2016). Our extrapolated DON values in the DS were 4.83 and 4.88 μmol/kg for AW and PW, respectively, and 4.05 μmol/kg for the DSOW (Table S1), in good agreement with Torres-Valdés et al. (2016), who reported DON concentrations close to 5 μmol/kg in the upper 100–200 m and fairly constant and slightly lower than 4 μmol/kg below.

3. Results and Discussion

3.1. Volume Transports in the eSPNA

The horizontal stream function of the depth-integrated volume transport illustrates the main features of the circulation across the OVIDE 2002 section (Figure 2a) described in detail elsewhere (Daniault et al., 2016; Lherminier et al., 2007). The basin-scale transport in the eSPNA was constituted by the northward flow of the NAC located at ~1,600 km from Greenland in the eastern rim of the gyre and by the southward flow of the EGC, in the western rim of the gyre along the Greenland slope. The intensity of both currents was ~30 Sv. The NAC flow carried 25.6 $\pm$ 1.4 Sv of waters corresponding to the density levels of the upper MOC limb (defined by the $\sigma_1 > 32.15$-kg/m^3 isopycnal, Lherminier et al., 2007), and a lower amount of lower limb waters (6.2 Sv). A fraction of the upper limb waters (9.8 Sv) circulated anticyclonically in the eastern end of the section (Figure 2a), while most of the flux fed the cyclonic subpolar gyre circulation. Part of it (~8.8 Sv) contoured anticyclonically the Reikjanes Ridge with the Iceland Current, and the rest flowed across the Reikjanes Ridge (Figure 1a). The Irminger Sea presented a cyclonic circulation. The eastern rim of this circulation was constituted by a northward flow with similar contributions of the Iceland Current and recirculation from the Labrador Sea (García-Ibáñez et al., 2015; Paillet et al., 1998). Finally, the subpolar gyre was closed by the southward flow of the EGC, carrying 3.6 Sv in the upper limb and 26.5 Sv in the lower limb of the MOC. Most of this flux corresponds with the Irminger SPMW (García-Ibáñez et al., 2015), the final product of the transformation of subtropical into SPMW along the eastern North Atlantic subpolar gyre, before entering the Labrador Sea.

Overall, 16.6 $\pm$ 1.1 and 5.3 $\pm$ 4.0 Sv of upper and lower limb waters flowed into the eSPNA through the Western Iberian basin (WEB), while 0.7 $\pm$ 1.4 and 21.4 $\pm$ 4.1 Sv, respectively, left the eSPNA through the Irminger and Iceland Basins (Figure 1a). Hence, the net transport across the OVIDE section was 16 Sv northward with the upper limb and southward with the lower limb of the MOC, respectively. At the GIS sills, 6.7 $\pm$ 0.6 Sv of upper limb waters continued northward, while approximately the same volume of dense overflow waters (3.5 $\pm$ 0.4 Sv of DSOW and 3.3 $\pm$ 0.5 Sv of ISOW) entered the eSPNA from the Nordic seas. Thus, the volume transport in the lower limb of the MOC increased from 6.7 Sv at the GIS sills to 16 Sv at the OVIDE section, implying a net formation of dense lower limb waters (i.e., overturning; García-Ibáñez et al., 2015) of 9.3 $\pm$ 1.3 Sv inside the eSPNA box (Figure 1a).
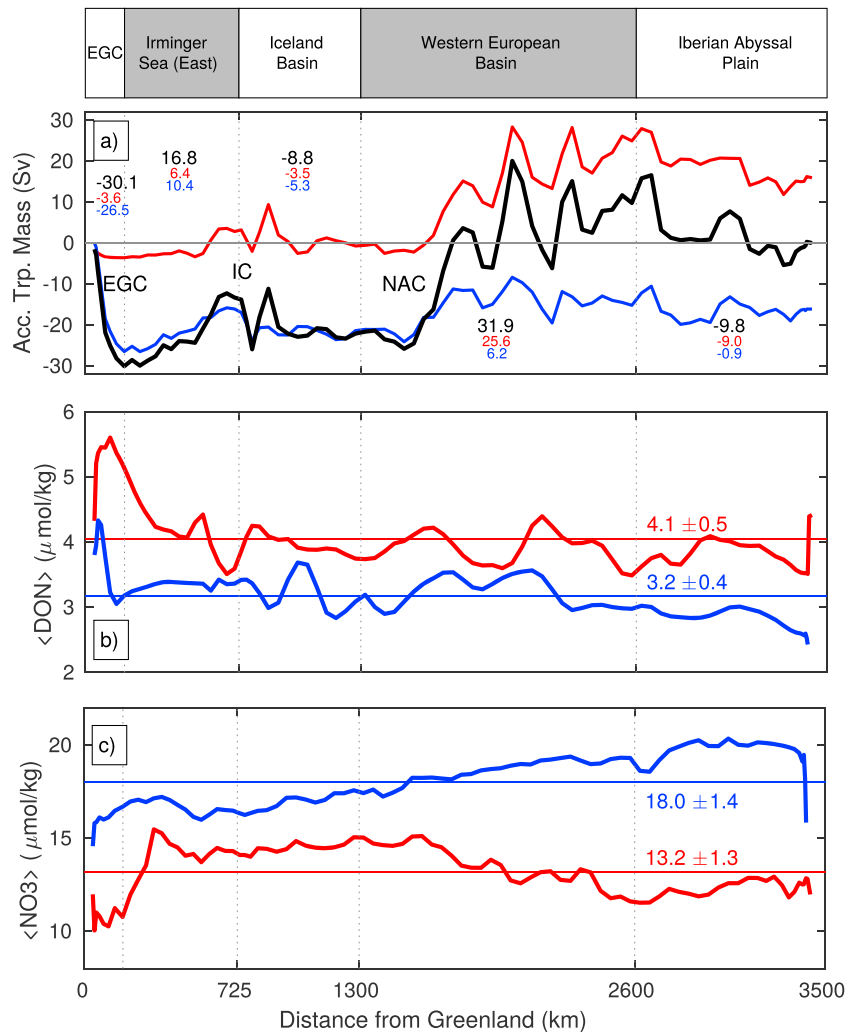
Figure 2. (a) Depth-integrated volume transports (1 Sv = 10^6 m³/s) across the OVIDE 2002 section horizontally accumulated from Greenland and distribution of the (b) dissolved organic nitrogen (DON) and (c) nitrate (NO₃) mean concentrations (μmol/kg) along the section. Transports and concentrations corresponding to the upper and lower limbs of the Meriodional Overturning Circulation, limited by the σ_1 = 32.15-kg/m³ isopycnal, are shown in red and blue colors, respectively. Net upper plus lower limb transports are represented by a black line. The horizontal red and blue lines and numbers in panels (b) and (c) represent the DON and nitrate section-mean concentrations for the upper and lower limbs. NAC, IC, and EGC represent the North Atlantic, Iceland, and East Greenland Currents. Integrated transports over the different regions are given in this order: total (larger font), upper limb (red), and lower limb (blue).

3.2. DON Transports Across the OVIDE 2002 Section

The transport of DON across the OVIDE 2002 section was calculated as the product of the volume transports and the DON concentrations (see section 2). As the net volume transport across the section has been previously subtracted in order to ensure volume conservation inside the box, the net transport is solely dependent on the spatial correlation between volume transports and DON concentrations. The section-mean DON concentrations were higher in the upper (4.1 ± 0.5μmol/kg) than in the lower limb of the MOC (3.2 ± 0.4μmol/kg; Figure 2b). The large-scale variability patterns along the section revealed little deviations from the section-mean except in the western Irminger Sea where strong positive anomalies were found in the upper and lower limbs.

The net northward DON transport in the WEB included 58 ± 4 and 19 ± 14 kmol/s in the upper and lower limbs of the MOC, respectively (Figure 1b). The net southward lower limb flux in the Irminger and Iceland Basins was 82 ± 14 kmol/s, dominated by the EGC, carrying DON-enriched waters with a transport-weighted mean concentration of 3.9 ± 0.1μmol/kg, significantly higher than the section mean. Although smaller

(7 ± 6 kmol/s), the southward flux of DON in the upper limb was also disproportionately large compared to the southward volume transport of 0.7 Sv. Due to this relative DON-enrichment in the western limit of the section, particularly in the Irminger Sea, the southward transport in the Irminger Sea and Iceland Basins exceeded the northward transport in the WEB, and the net DON flux across the OVIDE section was southward at a rate of 12 ± 3 kmol/s.

3.3. DON Budget in the SPNA: Net Production and Export by the MOC

The DON budget in the eSPNA was calculated as the balance of inputs minus outputs from the ocean, the rivers, and the atmosphere. The oceanic inputs minus outputs include the DON transports across the OVIDE 2002 section and the GIS sills (see section 2). At the GIS sills, the DSOW and ISOW transported 14 ± 4 and 13 ± 3 kmol/s of DON into the eSPNA, respectively, while the net upper limb flow was of 32 ± 5 kmol/s toward the Nordic Seas (Figure 1b). The resulting net DON flux through the northern boundary of the eSPNA was of 5 ± 5 kmol/s northward. The net balance of DON transports across the OVIDE 2002 section and the GIS sills resulted in a net export of 17 ± 6 kmol/s from the eSPNA. Furthermore, according to the global estimates of atmospheric nitrogen deposition (Jickells et al., 2017), 0.17–0.25 kmol/s (central value: 0.21 kmol/s) of DON are deposited annually into the eSPNA box. European, Iceland, and Greenland Rivers discharge 0.51–2.89 kmol/s of inorganic nitrogen to the eSPNA box (Sharples et al., 2016), while globally, the DON discharge by rivers represents 57% of the inorganic nitrogen flux (Kroeze et al., 2012). With this information, the riverine DON supply to the eSPNA is in the range 0.29–1.65 kmol/s (central value: ~1.0 kmol/s). Considering the DON fluxes across the OVIDE 2002 section, the GIS sills, the atmosphere, and the continents, we computed a net DON export of 16 ± 6 kmol/s from the eSPNA. This net export requires an equivalent net DON production of 16 ± 6 kmol/s (7.1 ± 2.6 TgN/year), in order to keep the steady state inside the box (equation **?**).

Our transport calculations reveal that 70–75% of the DON produced in the eSPNA (5.3 ± 1.3 TgN/year) is exported southward across the OVIDE 2002 section, carried by the southward-flowing lower limb waters of the EGC. The remaining smaller fraction (2.3 ± 1.3 TgN/year) is transported northward to the Nordic seas. DON is supplied to the eSPNA mainly by the waters of the upper limb of the MOC. In addition, local production of DON takes place in the surface layer of the eSPNA. Consequently, the DON transported to and produced in the upper limb of the MOC has to be transferred to the lower limb, that is, there should be an injection of DON from the surface to the deep ocean led by the overturning circulation. The DON vertical export associated with the MOC, calculated as the difference between the outputs (82 ± 14 kmol/s) and inputs (46 ± 13 kmol/s) to the eSPNA by lower limbs waters, was at least 36 ± 16 kmol/s (15.9 ± 7.1 TgN/year; Figure 1b). This figure represents a lower estimate because the possible remineralization within lower limb waters of the eSPNA was unresolved. Thus, up to one third (5.3 ± 1.3 TgN/year) of the DON exported to the deep ocean (> 15.9 ± 7.1 TgN/year) by the MOC is locally produced in the eSPNA.

3.4. Stoichiometry and Lability of the Produced DOM

The DON leaving the eSPNA with the EGC subsequently flows with the Western Greenland Current into the Labrador Sea where it joins the Deep Western Boundary Current (Cuny et al., 2002), being exported to the deep North Atlantic where it can contribute to remineralization processes in the ocean interior at lower latitudes (Carlson et al., 2010; Fontela et al., 2016). The bioavailability of the exported DOM determines its decay time scale and its potential to fuel heterotrophic activity downstream of the source region. Here we compute the stoichiometry of the produced dissolved organic materials and an upper-end estimate of their age as proxies of their lability.

The C:N ratio provides an indirect measure of bioavailability as fresh DOM has relatively low C:N ratios (~10), and aged DOM is progressively enriched in carbon, with respect to nitrogen (Hopkinson & Vallino, 2005). In order to obtain the C:N ratio of the DOM transported and cycled in the eSPNA, the DOC transports and budget were calculated following the same methodology used for DON (Figure S2). The C:N ratios of the transported and produced DOM were calculated as the ratio of the DOC and DON fluxes and net production rates.

The DOM imported into the eSPNA with the NAC had a C:N molar ratio of 15.4 ± 0.5, while the DOM exported from the Irminger Sea with the EGC and through the Iceland-Scotland ridge was characterized by lower C:N ratios, ~ 14.6 and 12 ± 2, respectively, indicating that the bulk C:N ratio of DOM entering the eSPNA with the NAC is reduced within this region (Figure 1b). This result is partly achieved by the supply of DOM with relatively low C:N (13.6–14.3) ratios from the overflows. Furthermore, according to our

DOC budget, 111 ± 45 kmolC/s were produced in the eSPNA, leading to a C:N molar ratio of 7.4 ± 4.1 for the locally produced DOM (Figure 1b). This ratio was only slightly higher than the Redfield proportion of recently produced particulate organic matter (6.7) and even slightly lower than the characteristic C:N ratios of bioavailable DOM (~ 10; Hopkinson & Vallino, 2005). This result suggests that, together with the import of DOM with relatively low C:N from the overflows, local production of fresh DON (with low C:N) reduces the C:N ratios of DOM in the eSPNA, before being exported away from the region, preferentially toward the deep ocean with the MOC.

The DON budget and the C:N ratios of organic matter production could be sensitive to the choice of the C:N ratio used to calculate DON concentrations at the GIS sills (r_{CN}). In order to rule out this possibility, an alternative calculation of the DON fluxes at the sills was performed with an upper estimate r_{CN} of 13 ± 2 (Hopkinson & Vallino, 2005). In this test, the net DON flux across the sills was 3 ± 3 kmol/s, and a net DON budget in the eSPNA, -14 ± 4 kmol/s. Both figures were very close to the values obtained with the initial proportion of $r_{CN} = 6.9 \pm 0.6$ (5 ± 5 and -16 ± 6 kmol/s, respectively; see Figure 1b). The alternative C:N ratio of DOM production (7.9 ± 4.1) was also practically unchanged. Therefore, the results are not significantly altered by the choice of the C:N ratio of the DOM in the GIS sills.

To further support the coherence of a low C:N ratio as indicator of DON lability, we estimated a transit time of 3 ± 1 years for a water parcel contouring the subpolar gyre in the eSPNA using a collection of Argo float trajectories (http://www.argo-france.fr/fr/home/; Figure S3). This transit time sets the upper limit for the age of the DON produced in the eSPNA at <3 years. This age is only slightly larger than the lifetime of semilabile DOM (~ 1.5 years) but significantly shorter than the lifetime of semirefractory DOM (~ 20 years; Hansell, 2013). The transit time is thus too short for the locally produced semirefractory DON to fully decay before being exported. Hence, the exported DON is at least semirefractory and can contain a potentially significant fraction of (semi)labile materials, as suggested by the low C:N ratio. Thus, the exported DOM has the potential to fuel heterotrophic processes in midlatitudes of the deep North Atlantic in the time scales of months to decades. This is consistent with several previous studies reporting important remineralization of DOM in the deep North Atlantic Ocean between polar and tropical latitudes (Carlson et al., 2010; Fontela et al., 2016; Hansell et al., 2012). In particular, Hansell et al. (2012) found the largest global rates of DOC removal from the deep ocean in the North Atlantic south of Greenland at $\sim 55°$ N, in the vicinity of the Labrador Sea and downstream of the EGC. It is a common view that the materials remineralized in the deep ocean at these latitudes are predominantly originated in the subtropical oceans and subduct with the MOC in the Labrador and Irminger Seas (Hansell et al., 2009). Our results suggest instead that relatively bioavailable DOM produced in the eSPNA could significantly contribute to explain the high rates of DOM remineralization in the North Atlantic.

3.5. The Contribution of DON to the Nitrogen Budget in the eSPNA

In this section, we compare the DON and the nitrate budgets in the region. To do so, the nitrate transports and budget were calculated following the same methodology as for DON. The nitrate transport in the upper limb of the MOC through the eastern part of the OVIDE 2002 section (the Western Iberian Basin) was 229 ± 15 kmol/s northward (Figure 1c), dominated by the NAC (Figure 2c), while the lower limb flux was 109 ± 75 kmol/s northward. The nitrate flux in the western part of the gyre (Iceland plus Irminger Basins) was 345 ± 71 kmol/s southward in the lower limb and nonsignificant in the upper limb (4 ± 20 kmol/s northward). The net nitrate transport across the OVIDE 2002 section was 3 ± 8 kmol/s southward.

The DSOW and ISOW transported 45 ± 5 and 46 ± 5 kmol/s of nitrate southward, respectively, into the eSPNA through the GIS sills, while the net northward flow of waters corresponding to the upper MOC limb carried 73 ± 13 kmol/s into the Nordic Seas (Figure 1c). This resulted in a net southward transport of 18 ± 15 kmol/s. Combining the fluxes across the OVIDE 2002 section and the sills, the net oceanic transport was 15 ± 14 kmol/s into the eSPNA box. According to the global estimates of atmospheric nitrogen deposition (Jickells et al., 2017), 0.02–0.03 gN·m^{-2}·year^{-1} and 0.06–0.09 gN·m^{-2}·year^{-1} are deposited annually in our study region in the form of ammonium and nitrate, respectively, adding up to a total flux of inorganic nitrogen of 0.68–1.0 kmol/s (central value: 0.8 kmol/s). The riverine supply of inorganic nitrogen was 0.51–2.89 kmol/s (central value: 1.7 kmol/s; Sharples et al., 2016). The riverine and atmospheric supplies (amounting 1.2–3.9 kmol/s in total) were added to the net nitrate input by the ocean circulation, summing up 17 ± 15 kmol/s (7.5 ± 6.6 TgN/year).

The net nitrate input into the eSPNA must be balanced by an equivalent net biological consumption (Figure 1c), reinforcing the observation of a net full-depth autotrophic balance in the eSPNA, in good agreement with previous studies in the area (Mazé et al., 2012; Zunino et al., 2015). Our budgets also show that the water column-integrated rates of net uptake of nitrate (7.5 ± 6.6 TgN/year) and net production of DON (7.1 ± 2.6 TgN/year) are roughly equivalent within error bars, such that the net nitrate consumption could be counterbalanced by net DON production. Torres-Valdés et al. (2013) computed a net deficit of nitrate in the Arctic Ocean and hypothesized that the nitrogen budget could be closed by a net import of DON. We found an opposite situation in the eSPNA, where our budget calculations indicate that the net nitrate import could end up as net DON production and export out of the region. Although subsequent studies failed to demonstrate the hypothesis of Torres-Valdés et al. (2013) for the Arctic Ocean (Torres-Valdés et al., 2016), our results reveal that DON production and export could represent a first-order contribution to the annual nitrogen budget in the eSPNA. Despite previous speculation and attempts (e.g., Álvarez et al., 2002; Torres-Valdés et al., 2016), to the best of our knowledge, this is the first time that in situ data are reported showing a distinct central contribution of DON to the nitrogen budget of an ocean basin.

Previous studies addressing the role of DOM in the biological carbon pump quantified either the contribution of DOC to net organic carbon export from the photic layer (Romera-Castillo et al., 2016; Roshan & DeVries, 2017) or to oxygen consumption in the dark ocean (Arístegui et al., 2002; Carlson et al., 2010; Fontela et al., 2016). All these studies found a consistent contribution of 17–40% of DOC to the carbon export from the surface or the respiration in the deep ocean. The budgets presented here differ from previous studies because they are integrated through the whole water column of the eSPNA and, therefore, do not capture the vertical export of materials from the euphotic zone but the net balance between production in the photic layer and remineralization in the deep ocean. If this balance is positive for net organic matter production, as it is the case, the fate of these materials is either burial in the sediments or/and horizontal export to other ocean regions. Despite sinking particles representing the major contribution to the export of organic matter from the euphotic zone in the eSPNA (Giering et al., 2014; Martin et al., 2011), sinking particulate material suffers remineralization in the mesopelagic and bathypelagic waters before reaching the sediments (Alkire et al., 2012; Lemaitre et al., 2018). As a consequence, the burial of organic nitrogen in the sediments of the open ocean (0.20 kmol/s; Brunnegård et al., 2004) and shelves (1.2 kmol/s; Wollast, 1993) is one order of magnitude lower than the net nitrate uptake computed here, and the organic nitrogen budget is then dominated by lateral fluxes of DON. Recent studies show that the transport of suspended material can also be important for the export of organic matter in different ocean basins (Baker et al., 2017). Due to the large error bars of our nitrate and DON budgets, we cannot discount the possibility that the lateral flux of suspended particulate nitrogen could also play a role in our study area.

The budgets presented here rely on mass transports and nutrient concentrations that were derived from climatological data in GIS sills but from a single-cruise realization in the OVIDE section. One must consider to which extent the biogeochemical rates are representative of the mean state of the eSPNA, as both currents and nutrient distributions can suffer significant interannual fluctuations (Mazé et al., 2012; Mercier et al., 2013). For the period 1997–2010, the mean MOC across the OVIDE section was 16 Sv with an interannual variation of ±1 Sv (SD of six realizations), and the mean amplitude of EGC and NAC was ∼ 30 Sv. During the OVIDE 2002 cruise, the amplitude of the MOC and these currents were very close to the climatological values of Mercier et al. (2013) and, thus, representative of the mean state of the system. The combined impact of the interannual variability of circulation and nutrient concentrations was assessed in Mazé et al. (2012). Those authors computed the nitrate, phosphate, and oxygen budgets using data from three different OVIDE occupations (2002, 2004, and 2006). They reported a mean nitrate consumption of −7.8 ± 6.5 and −8.4 ± 6.6 kmol/s in the Irminger Sea and the Iceland + Western European Basin, respectively, so that the total nitrate uptake was −16.2 kmol/s, in very good agreement with our estimate for 2002 (−17 ± 15 kmol/s). The authors also estimated the amplitude of the interannual variations of the nitrate flux across the OVIDE section at 7 kmol/s, not distinguishable from the mean state given the error bars. These evidences suggest that the budgets computed with the OVIDE 2002 cruise are representative of the mean state of the eSPNA in the early 21st century, at least within the reported error bars.

4. Conclusions

The eSPNA has long been recognized as a key region for vertical export of DOM into the deep ocean by the MOC. The DON and nitrate budgets presented here show that this region does not only act as a passive

belt transporting DOM originated in the subtropics, but it also behaves as a net autotrophic system, with a net production of DON at the expense of net nitrate uptake. The lower-limb waters enriched with relatively bioavailable DOM originated in the eSPNA are subsequently transported southward toward the Labrador Sea and the temperate North Atlantic, with potential impacts for the basin-scale microbial remineralization and biogeochemistry. The eSPNA is sensitive to natural climate variability and human-induced global change affecting both gyre-scale and overturning circulation (Smeed et al., 2018; Yashayaev et al., 2015) and primary production (Boyce et al., 2010; Zhang et al., 2018), which are intimately linked in this region (Johnson et al., 2013; Zhang et al., 2018). Understanding these interactions, and particularly the role of organic nutrients, is key to predict the evolution of the nitrogen cycle in the North Atlantic in the forthcoming decades.

References

Alkire, M. B., D'Asaro, E., Lee, C., Jane Perry, M., Gray, A., Cetinić, I., et al. (2012). Estimates of net community production and export using high-resolution, Lagrangian measurements of O2, NO3-, and POC through the evolution of a spring diatom bloom in the North Atlantic. *Deep-Sea Research I*, 64, 157–174. https://doi.org/10.1016/j.dsr.2012.01.012

Álvarez, M., Bryden, H. L., Pérez, F., Ríos, A. F., & Rosón, G. (2002). Physical and biogeochemical fluxes and net budgets in the subpolar and temperate North Atlantic. *Journal of Marine Research*, 60(1), 191–226.

Álvarez-Salgado, X. A., Nieto-Cid, M., Alvarez, M., Pérez, F. F., Morin, P., & Mercier, H. (2013). New insights on the mineralization of dissolved organic matter in central, intermediate, and deep water masses of the northeast North Atlantic. *Limnology and Oceanography*, 58(2), 681–696. https://doi.org/10.4319/lo.2013.58.2.0681

Arístegui, J., Duarte, C. M., Agustí, S., Doval, M., Alvarez-Salgado, X. A., & Hansell, D. A. (2002). Dissolved organic carbon support of respiration in the dark ocean. *Science*, 298, 1967. https://doi.org/10.1126/science.1076746

Baker, C. A., Henson, S. A., Cavan, E. L., Giering, S. L., Yool, A., Gehlen, M., et al. (2017). Slow-sinking particulate organic carbon in the Atlantic Ocean: Magnitude, flux, and potential controls. *Global Biogeochemical Cycles*, 31, 1051–1065. https://doi.org/10.1002/2017GB005638

Boyce, D. G., Lewis, M. R., & Worm, B. (2010). Global phytoplankton decline over the past century. *Nature*, 466(7306), 591–596. https://doi.org/10.1038/nature09268

Brambilla, E., & Talley, L. D. (2008). Subpolar mode water in the northeastern Atlantic: 1. Averaged properties and mean circulation. *Journal of Geophysical Research*, 113, C04025. https://doi.org/10.1029/2006JC004062

Brunnegård, J., Grandel, S., Ståhl, H., Tengberg, A., & Hall, P. O. (2004). Nitrogen cycling in deep-sea sediments of the porcupine abyssal plain, NE Atlantic. *Progress in Oceanography*, 63(4), 159–181. https://doi.org/10.1016/j.pocean.2004.09.004

Carlson, C. A. (2002). Production and removal processes. In D. A. Hansell & C. A. Carlson (Eds.), *Biogeochemistry of marine dissolved organic matter* (pp. 91–151). San Diego, CA: Academic Press.

Carlson, C., Ducklow, H., & Michaels, A. (1994). Annual flux of dissolved organic carbon from the euphotic zone in the northwestern Sargasso Sea. *Nature*, 371, 405–408.

Carlson, C. A., Hansell, D. A., Nelson, N. B., Siegel, D. A., Smethie, W. M., Khatiwala, S., et al. (2010). Dissolved organic carbon export and subsequent remineralization in the mesopelagic and bathypelagic realms of the North Atlantic basin. *Deep-Sea Research II*, 57(16), 1433–1445. https://doi.org/10.1016/j.dsr2.2010.02.013

Cuny, J., Rhines, P. B., Niiler, P. P., & Bacon, S. (2002). Labrador sea boundary currents and the fate of the Irminger Sea Water. *Journal of Physical Oceanography*, 32(2), 627–647. https://doi.org/10.1175/1520-0485(2002)032

Daniault, N., Mercier, H., Lherminier, P., Sarafanov, A., Falina, A., Zunino, P., et al. (2016). The northern North Atlantic Ocean mean circulation in the early 21st century. *Progress in Oceanography*, 146(July), 142–158. https://doi.org/10.1016/j.pocean.2016.06.007

Fontela, M., García-Ibáñez, M. I., Hansell, D. A., Mercier, H., & Pérez, F. F. (2016). Dissolved organic carbon in the North Atlantic Meridional Overturning Circulation. *Scientific Reports*, 6(November), 26931. https://doi.org/10.1038/srep26931

García-Ibáñez, M. I., Pardo, P. C., Carracedo, L. I., Mercier, H., Lherminier, P., Ríos, A. F., & Pérez, F. F. (2015). Structure, transports and transformations of the water masses in the Atlantic Subpolar Gyre. *Progress in Oceanography*, 135, 18–36. https://doi.org/10.1016/j.pocean.2015.03.009

Giering, S. L. C., Sanders, R., Lampitt, R. S., Anderson, T. R., Tamburini, C., Boutrif, M., et al. (2014). Reconciliation of the carbon budget in the ocean's twilight zone. *Nature*, 507, 480–483. https://doi.org/10.1038/nature13123

Hansell, D. A. (2013). Recalcitrant dissolved organic carbon fractions. *Annual Review of Marine Science*, 5(1), 421–445. https://doi.org/10.1146/annurev-marine-120710-100757

Hansell, D., Carlson, C. A., Repeta, D. J., & Schlitzer, R. (2009). Dissolved organic matter in the ocean: A Controversy stimulates new insights. *Oceanography*, 22(4), 202–11. https://doi.org/10.5670/oceanog.2009.109

Hansell, D. A., Carlson, C. A., & Schlitzer, R. (2012). Net removal of major marine dissolved organic carbon fractions in the subsurface ocean. *Global Biogeochemical Cycles*, 26, GB1016. https://doi.org/10.1029/2011GB004069

Hansen, B., Østerhus, S., Turrell, W. R., Jónsson, S., Valdimarsson, H., Hátún, H., & Olsen, S. M. (2008). The inflow of Atlantic Water, heat, and salt to the Nordic Seas across the Greenland-Scotland Ridge. In *Arctic-subarctic ocean fluxes* (pp. 15–43). Dordrecht, Netherlands: Springer. https://doi.org/10.1007/978-1-4020-6774-7_2

Henson, S. a., Sanders, R., Madsen, E., Morris, P. J., Le Moigne, F., & Quartly, G. D. (2011). A reduced estimate of the strength of the ocean's biological carbon pump. *Geophysical Research Letters*, 38, L04606. https://doi.org/10.1029/2011GL046735

Hopkinson, C., & Vallino, J. (2005). Efficient expert of carbon to the deep ocean through dissolved organic matter. *Nature*, 433(January), 142–145.

Jeansson, E., Olsen, A., Eldevik, T., Skjelvan, I., Omar, A. M., Lauvset, S. K., et al. (2011). The Nordic Seas carbon budget: Sources, sinks, and uncertainties. *Global Biogeochemical Cycles*, 25, GB4010. https://doi.org/10.1029/2010GB003961

Jickells, T. D., Buitenhuis, E., Altieri, K., Baker, A. R., Fennel, K., Kanakidou, M. ., et al. (2017). A re-evaluation of the magnitude and impacts of anthropogenic atmospheric nitrogen inputs on the ocean. *Global Biogeochemical Cycles*, 31, 289–305. https://doi.org/10.1002/2016GB005586

Jochumsen, K., Moritz, M., Nunes, N., Quadfasel, D., Larsen, K. M., Hansen, B., et al. (2017). Revised transport estimates of the Denmark Strait overflow. *Journal of Geophysical Research: Oceans*, 122, 3434–3450. https://doi.org/10.1002/2017JC012803

Johnson, C., Inall, M., & Häkkinen, S. (2013). Declining nutrient concentrations in the northeast Atlantic as a result of a weakening subpolar gyre. *Deep-Sea Research I*, *82*, 95–107. https://doi.org/10.1016/j.dsr.2013.08.007

Krauss, W. (1995). Currents and mixing in the Irminger Sea and in the Iceland Basin. *Journal of Geophysical Research*, *100*(C6), 10851. https://doi.org/10.1029/95JC00423

Kroeze, C., Bouwman, L., & Seitzinger, S. (2012). Modeling global nutrient export from watersheds. *Current Opinion in Environmental Sustainability*, *4*(2), 195–202. https://doi.org/10.1016/j.cosust.2012.01.009

Lemaitre, N., Planquette, H., Planchon, F., Sarthou, G., Jacquet, S., García-Ibáñez, M. I., et al. (2018). Particulate barium tracing of significant mesopelagic carbon remineralisation in the North Atlantic. *Biogeosciences*, *15*, 2289–2307. https://doi.org/10.5194/bg-15-2289-2018

Letscher, R. T., Hansell, D. A., Carlson, C. A., Lumpkin, R., & Knapp, A. N. (2013). Dissolved organic nitrogen in the global surface ocean: Distribution and fate. *Global Biogeochemical Cycles*, *27*, 141–153. https://doi.org/10.1029/2012GB004449

Lherminier, P., Mercier, H., Gourcuff, C., Alvarez, M., Bacon, S., & Kermabon, C. (2007). Transports across the 2002 Greenland-Portugal Ovide section and comparison with 1997. *Journal of Geophysical Research*, *112*, C07003. https://doi.org/10.1029/2006JC003716

Macrander, A., Send, U., Valdimarsson, H., Jónsson, S., & Käse, R. H. (2005). Interannual changes in the overflow from the Nordic Seas into the Atlantic Ocean through Denmark Strait. *Geophysical Research Letters*, *32*, L06606. https://doi.org/10.1029/2004GL021463

Martin, P., Lampitt, R. S., Jane Perry, M., Sanders, R., Lee, C., & D'Asaro, E. (2011). Export and mesopelagic particle flux during a North Atlantic spring diatom bloom. *Deep Sea Research I*, *58*(4), 338–349. https://doi.org/10.1016/J.DSR.2011.01.006

Mazé, G., Mercier, H., Thierry, V., Memery, L., Morin, P., & Pérez, F. F. (2012). Mass, nutrient and oxygen budgets for the northeastern Atlantic Ocean. *Biogeosciences*, *9*(10), 4099–4113. https://doi.org/10.5194/bg-9-4099-2012

McCartney, M. S., & Talley, L. D. (1982). The subpolar mode water of the north Atlantic Ocean. *Journal of Physical Oceanography*, *12*(11), 1169–1188. https://doi.org/10.1175/1520-0485(1982)012<1169:TSMWOT>2.0.CO;2

Mercier, H., Lherminier, P., Sarafanov, A., Gaillard, F., Daniault, N., Desbruyères, D., et al. (2013). Variability of the meridional overturning circulation at the Greenland-Portugal OVIDE section from 1993 to 2010. *Progress in Oceanography*, *132*, 250–261. https://doi.org/10.1016/j.pocean.2013.11.001

Nilsson, J., Björk, G., Rudels, B., Winsor, P., & Torres, D. (2008). Liquid freshwater transport and polar surface water characteristics in the east greenland current during the AO-02 Oden expedition. *Progress in Oceanography*, *78*(1), 45–57. https://doi.org/10.1016/j.pocean.2007.06.002

Østerhus, S., Turrell, W. R., Jónsson, S., & Hansen, B. (2005). Measured volume, heat, and salt fluxes from the Atlantic to the Arctic Mediterranean. *Geophysical Research Letters*, *32*, L07603. https://doi.org/10.1029/2004GL022188

Paillet, J., Arhan, M., & McCartney, M. S. (1998). Spreading of Labrador Sea Water in the eastern North Atlantic. *Journal of Geophysical Research*, *103*(C5), 10,223–10,239. https://doi.org/10.1029/98JC00262

Pickart, R. S., Straneo, F., & Moore, G. W. (2003). Is Labrador Sea water formed in the irminger basin? *Deep-Sea Research I*, *50*(1), 23–52. https://doi.org/10.1016/S0967-0637(02)00134-6

Piron, A., Thierry, V., Mercier, H., & Caniaux, G. (2017). Gyre-scale deep convection in the subpolar North Atlantic Ocean during winter 2014-2015. *Geophysical Research Letters*, *44*, 1439–1447. https://doi.org/10.1002/2016GL071895

Romera-Castillo, C., Letscher, R. T., & Hansell, D. A. (2016). New nutrients exert fundamental control on dissolved organic carbon accumulation in the surface Atlantic Ocean. *Proceedings of the National Academy of Sciences*, *113*(38), 10,497–10,502. https://doi.org/10.1073/pnas.1605344113

Roshan, S., & DeVries, T. (2017). Efficient dissolved organic carbon production and export in the oligotrophic ocean. *Nature Communications*, *8*(1), 2036. https://doi.org/10.1038/s41467-017-02227-3

Sharples, J., Middelburg, J. J., Fennel, K., & Jickells, T. D. (2016). What proportion of riverine nutrients reaches the open ocean? *Global Biogeochemical Cycles*, *31*, 39–58. https://doi.org/10.1002/2016GB005483

Smeed, D. A., Josey, S. A., Beaulieu, C., Johns, W. E., Moat, B. I., Frajka-Williams, E., et al. (2018). The North Atlantic Ocean is in a state of reduced overturning. *Geophysical Research Letters*, *45*, 1527–1533. https://doi.org/10.1002/2017GL076350

Torres-Valdés, S., Roussenov, V. M., Sanders, R., Reynolds, S., Pan, X., Mather, R., et al. (2009). Distribution of dissolved organic nutrients and their effect on export production over the Atlantic Ocean. *Global Biogeochemical Cycles*, *23*, GB4019. https://doi.org/10.1029/2008GB003389

Torres-Valdés, S., Tsubouchi, T., Bacon, S., Naveira-Garabato, A. C., Sanders, R., McLaughlin, F. A., et al. (2013). Export of nutrients from the Arctic Ocean. *Journal of Geophysical Research: Oceans*, *118*, 1625–1644. https://doi.org/10.1002/jgrc.20063

Torres-Valdés, S., Tsubouchi, T., Davey, E., Yashayaev, I., & Bacon, S. (2016). Relevance of dissolved organic nutrients for the Arctic Ocean nutrient budget. *Geophysical Research Letters*, *43*, 6418–6426. https://doi.org/10.1002/2016GL069245

Vidal, M., Aspillaga, E., Teixidor-Toneu, I., & Delgado-Huertas, A. (2018). Lateral transport of N-rich dissolved organic matter strengthens phosphorus deficiency in western subtropical North Atlantic. *Global Biogeochemical Cycles*, *32*, 1350–1366. https://doi.org/10.1029/2017GB005868

Wollast, R. (1993). Interactions of carbon and nitrogen cycles in the coastal zone. In *Interactions of C, N, P and S biogeochemical cycles and global change* (pp. 195–210). Berlin, Heidelberg: Springer Berlin Heidelberg. https://doi.org/10.1007/978-3-642-76064-8_7

Yashayaev, I., Seidov, D., & Demirov, E. (2015). A new collective view of oceanography of the Arctic and North Atlantic basins. *Progress in Oceanography*, *132*, 1–21. https://doi.org/10.1016/j.pocean.2014.12.012

Yashayaev, I., van Aken, H. M., Holliday, N. P., & Bersch, M. (2007). Transformation of the Labrador Sea water in the subpolar North Atlantic. *Geophysical Research Letters*, *34*, L22605. https://doi.org/10.1029/2007GL031812

Zhang, M., Zhang, Y., Shu, Q., Zhao, C., Wang, G., Wu, Z., & Qiao, F. (2018). Spatiotemporal evolution of the chlorophyll a trend in the North Atlantic Ocean. *Science of the Total Environment*, *612*, 1141–1148. https://doi.org/10.1016/j.scitotenv.2017.08.303

Zunino, P., Garcia-Ibañez, M. I., Lherminier, P., Mercier, H., Rios, A. F., & Pérez, F. F. (2014). Variability of the transport of anthropogenic CO2 at the Greenland-Portugal OVIDE section: Controlling mechanisms. *Biogeosciences*, *11*(8), 2375–2389. https://doi.org/10.5194/bg-11-2375-2014

Zunino, P., Lherminier, P., Mercier, H., Padín, X. A., Ríos, A. F., & Pérez, F. F. (2015). Dissolved inorganic carbon budgets in the eastern subpolar North Atlantic in the 2000s from in situ data. *Geophysical Research Letters*, *42*, 9853–9861. https://doi.org/10.1002/2015GL066243